Int. J. Heat Mass Transfer. Vol. 6, pp. 221–229. Pergamon Press 1963. Printed in Great Britain.

TRANSPORT PHENOMENA IN WEDGE FLOWS: PERTURBATION SOLUTIONS FOR SMALL MASS TRANSFER RATES

R. PROBER and W. E. STEWART
Chemical Engineering Department, University of Wisconsin, Madison, Wisconsin

Abstract—A perturbation method is used to obtain boundary-layer solutions for wedge flows with small mass transfer rates. Simple, explicit relations are obtained between the momentum, heat and mass transfer rates and the interfacial and free-stream conditions. Results are given for Prandtl and Schmidt numbers from zero to infinity, and for wedge geometries from $\beta = 1{\cdot}0$ to $\beta = -0{\cdot}163$.

NOMENCLATURE

The dimensions of each physical quantity are given in terms of mass (M), length (L), time (t) and temperature (T). Thus, energy has the dimensions ML^2t^{-2}. Any consistent units may be used.

$\hat{C}_p$, heat capacity of the fluid, $(ML^2t^{-2})M^{-1}T^{-1}$;

$\mathscr{D}_{AB}$, binary diffusivity, L^2t^{-1};

D_0, D_1, coefficients in equation (26), dimensionless;

D_0^*, D_1^*, values of D_0 and D_1 when $K = 0$;

F, G, integral functions introduced in (19), dimensionless;

K, dimensionless mass transfer rate defined in (4);

N_{A0}, N_{B0}, fluxes of species A and B into the boundary layer at $y = 0$, referred to co-ordinate axes fixed on the wall, moles $L^{-2}t^{-1}$;

R_v, R_T, R_{AB}, flux ratios defined in (1–3), dimensionless;

T_0, T_∞, wall and free-stream temperatures;

U, u_1x^m, magnitude of potential flow velocity next to the boundary layer, Lt^{-1};

X, $-K$, dimensionless;

a_v, f_0'' at given β with $K = 0$, dimensionless;

a_T, a_{AB}, Π_0' at given β and Λ with $K = 0$, dimensionless;

b_v, velocity-gradient perturbation g_0'', dimensionless;

b_T, b_{AB}, perturbation for gradient of temperature or concentration, dimensionless $= s_0'/\Lambda$;

c, molar density of fluid, moles L^{-3};

d_0, d_1, perturbations for the potential flow, defined in (29) and (30), dimensionless;

f, dimensionless stream function introduced by Hartree [4], [10] for wedge flows

$$= \left(\frac{2}{m+1}\,Uvx\right)^{-\frac{1}{2}} \int_{0,0}^{x,y} (u\,\mathrm{d}y - v\,\mathrm{d}x);$$

g, perturbation function for velocity, defined in (8), dimensionless;

h, k, functions substituted for g in integrating (12);

m, $\beta/(2-\beta)$, exponent in expression for U, dimensionless;

q_0, conductive heat flux into the boundary layer at $y = 0$, $(ML^2t^{-2})L^{-2}t^{-1}$;

s, perturbation function for temperature or concentration, defined in (9), dimensionless;

u, v, fluid velocity components in x- and y-directions;

$x_{A0}, x_{A\infty}$, mole fractions of species A in the fluid next to the wall and in the free stream;

x, distance downstream from leading edge or stagnation point;

y, distance from the wedge surface, measured normal to it.

Greek symbols

A, Prandtl number (A_T) or Schmidt number (A_{AB});

Π, dimensionless temperature $(T - T_0)/(T_\infty - T_0)$, or dimensionless composition $(x_A - x_{A0})/(x_{A\infty} - x_{A0})$;

β, wedge angle in radians;

η, dimensionless co-ordinate introduced by Hartree [4], [10] for wedge flows

$$= y\sqrt{\left(\frac{m+1}{2}\frac{U}{\nu x}\right)};$$

ν, kinematic viscosity of the fluid, L^2t^{-2};

ρ, density of the fluid, ML^{-3};

τ_0, wall shear stress, $(MLt^{-2})L^{-2}$.

Superscripts

$'$, $\frac{\partial}{\partial\eta}$;

$*$, denotes a quantity evaluated at $K = 0$.

Subscripts

0, denotes a quantity evaluated at $\eta = 0$;

∞, denotes a quantity evaluated at $\eta \to \infty$;

A or B, denotes chemical species A or B in a binary mixture;

T, temperature;

v, velocity.

Functions

erf (a), $\frac{2}{\sqrt{(\pi)}}\int_0^a e^{-x^2}\,dx = -\text{erf}\,(-a)$;

$O(X^2)$, terms of second and higher degree in X.

1. INTRODUCTION

In an earlier paper [1] the authors gave exact solutions for simultaneous heat transfer and diffusion in wedge flows with various mass transfer rates. Procedures were described there for solving various mass transfer problems by direct or inverse interpolation of the tabulated solutions. The purpose of the present paper is to give simpler solutions for the region of small mass transfer rates, by treating the effects of mass transfer as small perturbations. In these new solutions the results are expressed as analytic functions of the mass transfer rate; this allows rapid, accurate calculation of many types of mass transfer problems.

The perturbation solutions given here for wedge flows are extensions of those given by Merk [2] for the flat-plate geometry. The present work was undertaken to obtain information on flows with pressure gradient, and to determine the influence of the Prandtl and Schmidt numbers more completely.

The nomenclature of Paper [1] is retained here, with some additions. Here again, mass transfer is defined as the transport of matter through an interface or porous wall. Diffusion is defined as the relative motion of different chemical species in a mixture. This terminology is useful because of the mathematical similarities that exist between mass transfer processes in pure fluids (boundary-layer control, condensation of pure vapors, etc.) and in mixtures.

The development of the solutions is discussed in Sections 2, 3, and 4. The use of the results is discussed in Section 5.

2. GOVERNING EQUATIONS

Consider the steady two-dimensional flow of a pure or binary fluid across a symmetrical wedge of included angle $\pi\beta$ radians. (A physical model for the case of negative β is given in [1].) The physical properties are assumed constant and dissipation, radiation and chemical reaction are neglected. The interfacial fluid conditions T_0 and x_{A0} are constant, and *one* of the following four quantities (R_v, R_T, R_{AB} or K) is specified as a constant along the surface:

$$R_v = \frac{v_0\rho U}{\tau_0} \tag{1}$$

$$R_T = \frac{v_0 \rho \hat{C}_p (T_0 - T_\infty)}{q_0} \tag{2}$$

$$R_{AB} = \frac{v_0 c (x_{A0} - x_{A\infty})}{-c\mathscr{D}_{AB}\left(\frac{\partial x_A}{\partial y}\right)_0} = \frac{x_{A0} - x_{A\infty}}{\left(\frac{N_{A0}}{N_{A0} + N_{B0}} - x_{A0}\right)} \tag{3}$$

$$K = \frac{v_0}{U}\sqrt{\left(\frac{2}{m+1}\frac{Ux}{\nu}\right)} \tag{4}$$

where $U = u_1 x^m$ is the potential flow velocity adjacent to the boundary layer.

It is shown in [1] that *all four* of the quantities R_v, R_T, R_{AB} and K are constant along the surface under the above conditions, and that the boundary-layer processes are then described by the equations

$$f''' + ff'' + \beta(1 - f'^2) = 0 \tag{5}$$

$$\Pi'' + \Lambda f \Pi' = 0 \tag{6}$$

with the boundary conditions:

$$\left.\begin{array}{ll} \text{at } \eta = 0: & f = X, f' = 0, \Pi = 0 \\ \text{as } \eta \to \infty: & f' \to 1, \Pi \to 1. \end{array}\right\} \tag{7}$$

Here, as in [1], Π may represent the dimensionless temperature Π_T or the dimensionless concentration Π_{AB}; Λ correspondingly represents the Prandtl number Λ_T or the Schmidt number Λ_{AB}. The quantity $X = -K$ is used in (7) to avoid sign difficulties in the following development.

We now consider the solutions of (5), (6) and (7) for small values of X. Expansion of f and Π in powers of X gives:

$$f(\eta, \beta, X) = f^*(\eta, \beta) + Xg(\eta, \beta) + O(X^2) \tag{8}$$

$$\Pi(\eta, \beta, X, \Lambda) = \Pi^*(\eta, \beta, \Lambda) + Xs(\eta, \beta, \Lambda) + O(X^2). \tag{9}$$

The functions f^* and Π^* are the solutions of (5), (6) and (7) at $X = 0$; these are well known [3, 4, 5, 6, 1] and need not be discussed here. The pertubation functions, g and s, are the first partial derivatives of f and Π with respect to X, evaluated at $X = 0$; these perturbation functions are the subject of the present work. The terms X^2, X^3, etc. are not considered here; at small values of X they are unimportant, and at large values of X the solutions given in [1] are more convenient.

Differentiation of (8) and (9) yields the corresponding formulae for the derivatives of f and Π:

$$\left.\begin{array}{l} f' = f'^* + Xg' + O(X^2) \\ f'' = f''^* + Xg'' + O(X^2) \\ f''' = f'''^* + Xg''' + O(X^2) \end{array}\right\} \tag{10}$$

$$\left.\begin{array}{l} \Pi' = \Pi'^* + Xs' + O(X^2) \\ \Pi'' = \Pi''^* + Xs'' + O(X^2) \end{array}\right\} \tag{11}$$

Here, as before, the notation (′) indicates partial differentiation with respect to η at constant β, X, Λ.

Equations (5), (6) and (7) can now be rewritten in terms of the expansions of f and Π, for a small but arbitrary value of X. This yields the expected set of equations for f^* and Π^*, plus the following set of equations for g and s:

$$g''' + f^* g'' - 2\beta f'^* g' + f''^* g = 0 \tag{12}$$

$$s'' + \Lambda f^* s' + \Lambda g \Pi'^* = 0. \tag{13}$$

The boundary conditions on g and s are:

$$\begin{array}{ll} \text{at } \eta = 0; & g = 1, g' = 0, s = 0 \\ \text{as } \eta \to \infty; & g' \to 0, s \to 0. \end{array} \tag{14}$$

Equations (12), (13) and (14) are solvable numerically for $g(\eta, \beta)$ and $s(\eta, \beta, \Lambda)$, once the functions $f^*(\eta, \beta)$ and $\Pi^*(\eta, \beta, \Lambda)$ have been calculated at the specified β and Λ.

The equations for g include two-point boundary conditions. To obtain simpler boundary conditions, we utilize the linearity of (12) and express g as follows:

$$g = h + g_0'' k. \tag{15}$$

Here h and k are solutions of (12) under the boundary conditions

$$\begin{array}{lll} h(0) = 1 & h'(0) = 0 & h''(0) = 0 \\ k(0) = 0 & k'(0) = 0 & k''(0) = 1. \end{array} \tag{16}$$

After evaluating the functions $h(\eta, \beta)$ and $k(\eta, \beta)$, the constant $g''(0)$ can be found by application of (14) and (15):

$$g_0'' = \lim_{\eta \to \infty} (-h'/k'). \tag{17}$$

The g-profile can then be calculated from the

h and k functions according to (15). This method was used in all of the solutions for g reported here.

The calculation of s also involves two-point boundary conditions, and can be similarly treated; however, it is simpler to work with the general solution of (6) and (7):

$$\Pi = \frac{\int_0^\eta \exp(-\Lambda \int_0^\eta f\,\mathrm{d}\eta)\,\mathrm{d}\eta}{\int_0^\infty \exp(-\Lambda \int_0^\eta f\,\mathrm{d}\eta)\,\mathrm{d}\eta}. \tag{18}$$

Differentiation of this solution with respect to X, and application of (9), gives:

$$s = \frac{\int_0^\eta -\Lambda G \exp(-\Lambda F)\,\mathrm{d}\eta}{\int_0^\infty \exp(-\Lambda F)\,\mathrm{d}\eta} + \frac{[\int_0^\eta \exp(-\Lambda F)\,\mathrm{d}\eta][\int_0^\infty \Lambda G \exp(-\Lambda F)\,\mathrm{d}\eta]}{[\int_0^\infty \exp(-\Lambda F)\,\mathrm{d}\eta]^2} \tag{19}$$

in which the notations F and G represent the functions $\int_0^\eta f^*\,\mathrm{d}\eta$ and $\int_0^\eta g\,\mathrm{d}\eta$, respectively. Thus the function $s(\eta, \beta, \Lambda)$ can be found by quadrature for any specified value of Λ once the functions $f^*(\eta, \beta)$ and $g(\eta, \beta)$ are known at the given value of β.

The temperature and concentration gradients at the wall are of special importance, and can be obtained easily from the derivatives of the above results with respect to η:

$$\Pi'(0) = \frac{1}{\int_0^\infty \exp(-\Lambda \int_0^\eta f\,\mathrm{d}\eta)\,\mathrm{d}\eta} \tag{20}$$

$$s'(0) = \frac{\Lambda \int_0^\infty G \exp(-\Lambda F)\,\mathrm{d}\eta}{[\int_0^\infty \exp(-\Lambda F)\,\mathrm{d}\eta]^2}. \tag{21}$$

Equation (21) is also obtainable from (20) by differentiating with respect to X. Equations (19) and (21) were previously derived by Merk [2] in his perturbation studies of the flat-plate geometry ($\beta = 0$).

3. NUMERICAL SOLUTIONS

Numerical solutions for the perturbation functions were calculated over the region

$$-0{\cdot}16279 \le \beta \le 1{\cdot}0$$

$$0{\cdot}1 \le \Lambda \le 100.$$

The computational procedures used are described in [7]. The main results are presented in Table 1 and Figs. 1–4. For convenience, the unperturbed functions $f_0''^*$ and $\Pi_0''^* \Lambda^{-1/3}$ are given in Table 2 for the same values of β and Λ. The values for $\Lambda \to 0$ and $\Lambda \to \infty$ were found analytically as described in Section 4.

Table 1. Exact solutions of the perturbation equations

		b_T or $b_{AB} = s_0'/\Lambda$										
β	$b_v = g_0''$	$\Lambda \to 0$	$\Lambda = 0{\cdot}1$	$\Lambda = 0{\cdot}2$	$\Lambda = 0{\cdot}5$	$\Lambda = 0{\cdot}7$	$\Lambda = 1{\cdot}0$	$\Lambda = 2$	$\Lambda = 5$	$\Lambda = 10$	$\Lambda = 100$	$\Lambda \to \infty$
1·0	0·575	0·787	0·705	0·685	0·656	0·646	0·636	0·618	0·600	0·590	0·574	0·566
0·5	0·599	0·880	0·751	0·720	0·680	0·666	0·652	0·628	0·605	0·593	0·574	0·566
0·0	0·723	1·308	0·948	0·874	0·783	0·752	0·723	0·676	0·632	0·610	0·577	0·566
−0·1	0·855	1·741	1·141	1·025	0·884	0·838	0·795	0·726	0·661	0·629	0·580	0·566
−0·162793	1·168	2·757	1·580	1·369	1·117	1·038	0·963	0·843	0·732	0·676	0·591	0·566

Table 2. Exact boundary layer solutions at $K = 0$

		$a_T \Lambda_T^{-1/3}$ or $a_{AB} \Lambda_{AB}^{-1/3} = \Pi_0'^* \Lambda^{-1/3}$									
β	$a_v = f_0''^*$	$\Lambda = 0{\cdot}1$	$\Lambda = 0{\cdot}2$	$\Lambda = 0{\cdot}5$	$\Lambda = 0{\cdot}7$	$\Lambda = 1{\cdot}0$	$\Lambda = 2$	$\Lambda = 5$	$\Lambda = 10$	$\Lambda = 100$	$\Lambda \to \infty$
1·0	1·2326	0·4728	0·5067	0·5460	0·5584	0·5704	0·5901	0·6098	0·6207	0·6434	0·6608
0·5	0·9277	0·4592	0·4883	0·5202	0·5298	0·5389	0·5534	0·5672	0·5746	0·5896	0·6011
0·0	0·4696	0·4266	0·4452	0·4620	0·4662	0·4696	0·4740	0·4769	0·4780	0·4789	0·4790
−0·1	0·3193	0·4103	0·4240	0·4341	0·4358	0·4368	0·4368	0·4349	0·4329	0·4272	0·4212
−0·162793	0·1832	0·3910	0·3993	0·4020	0·4010	0·3993	0·3943	0·3866	0·3809	0·3662	0·3500

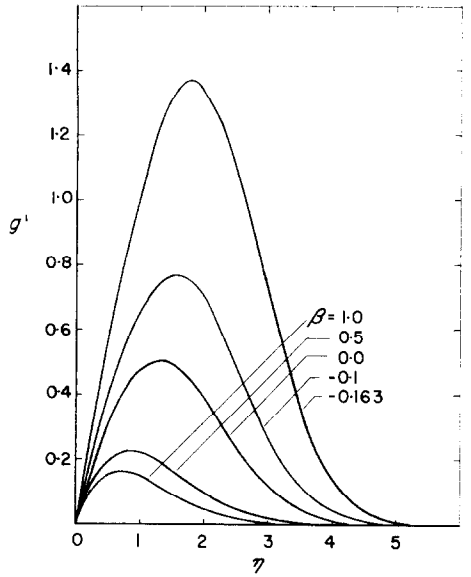

FIG. 1. Profiles of the velocity perturbation g'.

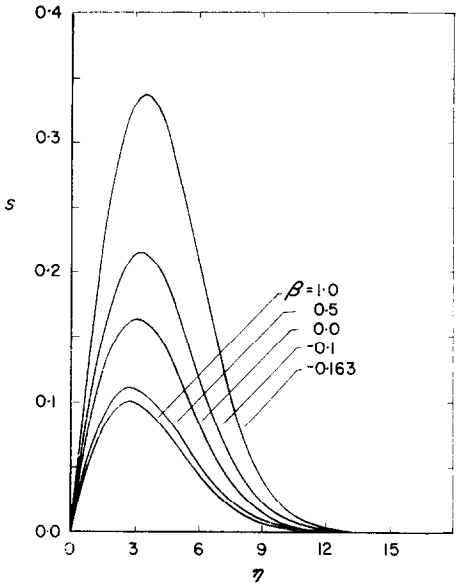

FIG. 2a. Profiles of the temperature or concentration perturbation, s, at $\Lambda = 0{\cdot}1$.

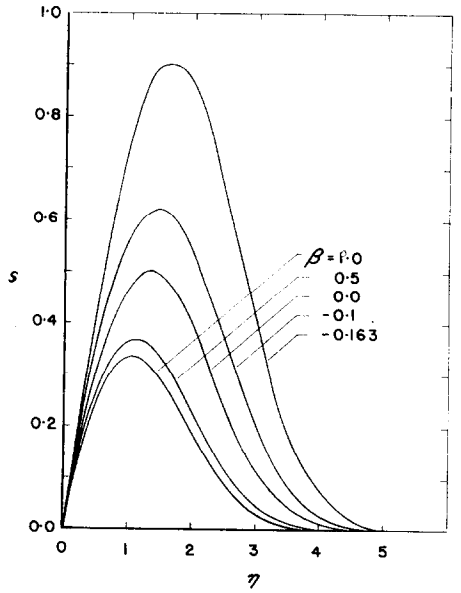

FIG. 2b. Profiles of s at $\Lambda = 1$.

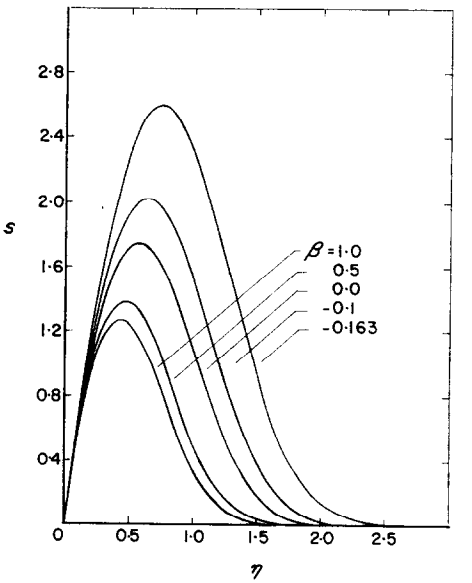

FIG. 2c. Profiles of s at $\Lambda = 10$.

P

The perturbations of the temperature, concentration and longitudinal velocity are plotted in Figs. 1 and 2 as functions of η. It is clear that the perturbations reach a maximum in the middle of the boundary layer, and vanish asymptotically in the potential flow. Furthermore, the fact that both g' and s are positive or zero everywhere indicates that for $X > 0$ (mass transfer toward the wall) the local values of f' and Π in the boundary layer are increased. These results are consistent with known solutions of the boundary-layer equations for larger values of X.

The effects of mass transfer on the velocity, temperature and concentration gradients at the wall are shown in Table 1 and Figs. 3 and 4. The influence of the flow geometry is small except in the neighborhood of $\beta = -0{\cdot}19884$; trial calculations suggest that the perturbations become infinite at this point.

The results for $g''(0)$ and $s'(0)$ for $\Lambda \geq 0{\cdot}1$ are believed accurate within 0·5 in the last digit. This is indicated by comparison of the values at $\Lambda = 100$, which are the most difficult to compute numerically, with asymptotic calculations given in the next section. Also, our results for $\beta = 0$ and $\Lambda \geq 1$ agree closely with values given by Merk [2].

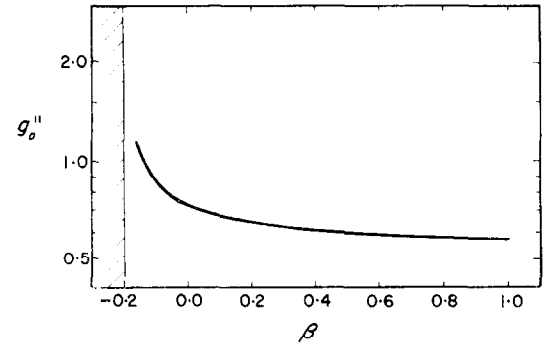

FIG. 3. Perturbation of the velocity gradient at the wall. The shaded region includes separated and unsteady flows.

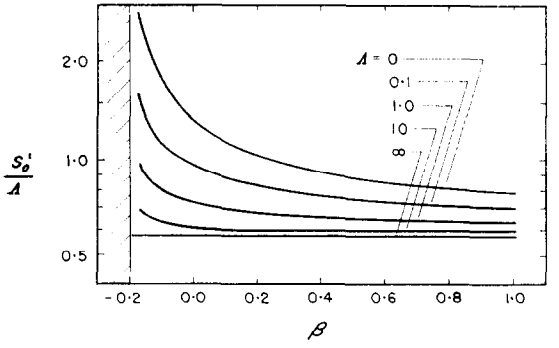

FIG. 4. Perturbations of the temperature gradient and concentration gradient at the wall. The shaded region includes separated and unsteady flows.

4. ASYMPTOTIC SOLUTIONS

The s function (temperature or concentration perturbation) can be calculated analytically without much difficulty if Λ is not too near unity. Here we consider only the calculation of s_0', by asymptotic integration of (21).

4a. *Solution for large* Λ

Here the temperature or concentration boundary layer is thin, so that it is feasible to represent F and G in (21) by their Maclaurin expansions:

$$F = \eta f_0^* + \tfrac{1}{2}\eta^2 f_0'^* + \tfrac{1}{6}\eta^3 f_0''^* + \tfrac{1}{24}\eta^4 f_0'''^* + \ldots$$
$$= \tfrac{1}{6}\eta^3 f_0''^* - \tfrac{1}{24}\eta^4\beta + \tfrac{1}{120}\eta^6(2\beta - 1)(f_0''^*)^2 + \ldots \quad (22)$$

$$G = \eta g_0 + \tfrac{1}{2}\eta^2 g_0' + \tfrac{1}{6}\eta^3 g_0'' + \tfrac{1}{24}\eta^4 g_0''' + \ldots$$
$$= \eta + \tfrac{1}{6}\eta^3 g_0'' - \tfrac{1}{24}\eta^4 f_0''^* + \tfrac{1}{120}\eta^5\beta + \ldots \quad (23)$$

Insertion of these truncated series in the numerator of (21) gives, after a partial expansion of the exponential function:

$$\int_0^\infty G \exp(-\Lambda F)\, d\eta$$
$$= \int_0^\infty \left(\eta + \tfrac{1}{6}\eta^3 g_0'' - \ldots\right) \exp\left(-\frac{\Lambda}{6}\eta^3 f_0''^*\right)$$
$$\left(1 - \frac{\Lambda}{24}\eta^4\beta + \frac{\Lambda^2}{1152}\eta^8\beta^2 + \ldots\right) d\eta. \quad (24)$$

It should be noted that this equation is meaningful only for $f_0''^* > 0$, that is, for $\beta > -0{\cdot}19884$.

Equation (24) can be integrated easily to give a series in terms of gamma functions, and the denominator of (21) can be evaluated in the

same way. Then taking the ratio of the two series, one obtains the asymptotic expansion:

$$\frac{s'(0)}{\Lambda} \simeq 0{\cdot}56605 + 0{\cdot}01659\,\frac{\beta}{(f_0''^*)^{4/3}\Lambda^{1/3}} + 0{\cdot}20543\,\frac{g_0''}{(f_0''^*\Lambda)^{2/3}} + 0{\cdot}01428\,\frac{\beta^2}{(f_0''^*)^{8/3}\Lambda^{2/3}} - 0{\cdot}09434\,\frac{1}{\Lambda} + 0{\cdot}01427\,\frac{\beta^3}{(f_0''^*)^4\Lambda} + 0{\cdot}09434\,\frac{g_0''\beta}{(f_0''^*)^2\Lambda} - 0{\cdot}006289\,\frac{(2\beta-1)}{\Lambda} + \ldots \qquad (25)$$

This solution can also be obtained, with somewhat greater difficulty, by differentiating the asymptotic series for $1/\Pi'(0, \beta, K, \Lambda)$ given in (56) of [1]. When $\beta = 0$, (25) yields the dominant terms of Merk's asymptotic series [2] for the flat plate.

The accuracy of (25) is shown in Table 3. The accuracy is best for large Λ and positive β, as expected. At $\beta = -0{\cdot}19884$ the series becomes meaningless, as noted above; however, the series remains valid for large Λ at all higher values of β.

Table 3. Accuracy of equation (25)

β	Λ	Per cent error in b_T or b_{AB}: equation (25), 1 term	equation (25), 4 terms	equation (25), 8 terms
1·0	0·5	−13·7	15·5	− 2·4
	1·0	−11·0	8·5	− 0·8
	10	− 4·1	1·0	0·0
	100	− 1·3	0·1	0·0
0·0	0·5	−27·7	22·2	− 0·3
	1·0	−21·8	12·2	0·1
	10	− 7·2	1·4	0·0
	100	− 1·9	0·1	0·0
−0·162793	0·5	−49·4	58·3	−62·5
	1·0	−41·2	36·9	−33·2
	10	−16·3	6·7	− 3·2
	100	− 4·2	0·9	− 0·2

4b. *Solution for small Λ*

For small values of Λ the thermal or diffusional boundary layer extends well into the potential flow, where the flow conditions are given by:

$$\int_0^\eta f\,d\eta = D_0 - D_1\eta + \tfrac{1}{2}\eta^2. \qquad (26)$$

Here D_0 and D_1 are functions of β and K; numerical values are given in [1] and in Table 4.

Table 4. Velocity profile constants for the perturbed potential flow

β	D_0^*	D_1^*	d_0	d_1
1·0	0·3681	0·6500	−0·244	−1·237
0·5	0·5327	0·8048	−0·462	−1·383
0·0	1·0914	1·2168	−1·662	−2·054
−0·1	1·4558	1·4427	−3·033	−2·735
−0·162793	1·9628	1·7252	−6·478	−4·330

Insertion of (26) in (20) gives the asymptotic solution:

$$\Pi'(0) \leq \left(\frac{2\Lambda}{\pi}\right)^{1/2} \frac{\exp\,(D_0\Lambda - \tfrac{1}{2}D_1^2\Lambda)}{[1 + \operatorname{erf} D_1\sqrt{(\tfrac{1}{2}\Lambda)}]}. \qquad (27)$$

This solution is quite accurate for $\Lambda \leq 0{\cdot}1$, over a wide range of K, as shown in [1]. The inequality in (27) arises from the fact that (26) overestimates $\int_0^\eta f\,d\eta$ within the velocity boundary layer.

A perturbation formula for small Λ can be obtained by differentiation of (27) with respect to X:

$$\frac{s'(0)}{\Lambda} \simeq \left(\frac{2\Lambda}{\pi}\right)^{1/2} \frac{(d_0 - D_1^* d_1)\exp\,(D_0^*\Lambda - \tfrac{1}{2}D_1^{*2}\Lambda)}{[1 + \operatorname{erf} D_1\sqrt{(\tfrac{1}{2}\Lambda)}]} - \frac{2}{\pi}\,d_1\,\frac{\exp\,(D_0^*\Lambda - D_1^{*2}\Lambda)}{[1 + \operatorname{erf} D_1^*\sqrt{(\tfrac{1}{2}\Lambda)}]} \qquad (28)$$

in which

$$d_1 = \left.\frac{\partial D_1}{\partial X}\right|_{X=0} = -g(\infty) \qquad (29)$$

and

$$d_0 = \left.\frac{\partial D_0}{\partial X}\right|_{X=0} = \int_0^\infty [g - g(\infty)]\,d\eta. \qquad (30)$$

Values of D_0^*, D_1^*, d_0 and d_1 are given in Table 4.

The accuracy of (28) is tested in Table 5.

Table 5. Accuracy of equation (28)

β	Λ	b, equation (28)	b, exact
1·0	0·1	0·703	0·705
0·5	0·1	0·743	0·751
0·0	0·1	0·913	0·948
−0·1	0·1	1·073	1·141
−0·162793	0·1	1·430	1·580

The agreement is quite good except near the separation region.

In the limit as $\Lambda \to 0$, (28) becomes exact, and gives:

$$\lim_{\Lambda \to \infty} \frac{s'(0)}{\Lambda} = -\frac{2d_1}{\pi}. \tag{31}$$

Values computed from this equation are included in Table 1 and in Fig. 4. It is interesting that these values depend strongly on the wedge angle β, whereas the asymptote at $\Lambda \to \infty$ is independent of β (for $\beta > -0{\cdot}19884$).

5. CALCULATION OF INTERPHASE TRANSFER

Transfer calculations are easily carried out with the information in Tables 1 and 2. Thus, if K is known (recall that $X \equiv -K$) one can calculate the dimensionless velocity, temperature and concentration gradients directly according to (10) or (11). If K is unknown, one of the flux ratios R will normally be known, and the mass transfer rate can be found by solving for K in one of the following equations:

$$\frac{K}{a_v} = \frac{R_v}{1 + b_v R_v} \tag{32a}$$

$$\frac{K\Lambda_T}{a_T} = \frac{R_T}{1 + b_T R_T} \tag{32b}$$

$$\frac{K\Lambda_{AB}}{a_{AB}} = \frac{R_{AB}}{1 + b_{AB} R_{AB}}. \tag{32c}$$

Once K has been determined from one of these equations, the other two equations can be solved directly for the flux ratios. Equations (32) thus give direct solutions for the four quantities R_v, R_T, R_{AB}, and K, when any one of the four is specified. A great variety of practical problems can be solved directly in this way; [8] and [9] indicate some of the possibilities.

The accuracy of (32a, b, c) is tested in Table 6, by comparison with exact solutions from [1]. Good agreement is obtained for a considerable range of R, except near the separation region.

Table 6. Accuracy of equations (32b, c)

		Percent error in predicted K		
β	R	$\Lambda = 0{\cdot}1$	$\Lambda = 1{\cdot}0$	$\Lambda = \infty$
1·0	−0·5	−8·4	−5·6	−4·1
	−0·25	−1·0	−1·0	0·7
	0·0	0·0	0·0	0·0
	0·25	−0·4	−0·7	−0·4
	0·50	−2·0	−2·3	−1·4
0·0	−0·5	+4·1	−5·9	−4·1
	−0·25	+1·6	−1·0	0·7
	0·0	0·0	0·0	0·0
	0·25	+1·2	−0·3	−0·4
	0·5	+5·2	−1·7	−1·4
−0·16279	−0·5	+139.1	+5·1	−4·1
	−0·25	+20·1	+1·4	−0·7
	0·0	0·0	0·0	0·0
	0·25	—	3·8	−0·4
	0·50	—	—	−1·4
−0·16279	Separation	+6·5 ($R = 0{\cdot}0647$)	+10·9 ($R = 0{\cdot}379$)	−100·0 ($R = \infty$)

Thus, (32a, b, c) should prove very useful for calculation of momentum, heat and mass transfer on wedge-like surfaces.

The results given here for wedge flows can be applied easily to various two-dimensional and axisymmetric geometries. A variety of approximate methods are available for making such transformations, and we will not attempt to discuss their relative merits here. The results found here at $\Lambda = \infty$ have been found to hold also in non-separated three-dimensional flows; this will be treated by one of us in a forthcoming paper.

Applications of these results to systems with variable physical properties, and to mixtures of more than two components, will be presented in later papers of this series.

ACKNOWLEDGEMENT

This work was supported by the Sinclair Refining Company and the Wisconsin Alumni Research Foundation. This support is gratefully acknowledged.

REFERENCES

1. W. E. STEWART and R. PROBER, Heat transfer and diffusion in wedge flows with rapid mass transfer, *Int. J. Heat Mass Transfer*. To be published.
2. H. J. MERK, Mass transfer in laminar boundary layers calculated by means of a perturbation method, *Appl. Sci. Res.* **A8**, 237 (1959).
3. V. M. FALKNER and S. W. SKAN, Some approximate solutions of the laminar boundary layer equations. Aero. Res. Council (Gt. Brit.) ARC R & M 1314 (1930); *Phil. Mag.* **12**, 865 (1931).
4. D. R. HARTREE, On an equation occurring in Falkner and Skan's approximate treatment of the equations of the boundary layer, *Proc. Camb. Phil. Soc.* **33**, Part II, 223 (1937).
5. E. R. G. ECKERT, Die Berechnung des Wärmeübergangs in der laminaren Grenzschicht. *V.D.I.-Forschungsheft*, 416 (1942).
6. H. J. MERK, Rapid calculations for boundary-layer transfer using wedge solutions and asymptotic expansions, *J. Fluid Mech.* **5**, 460 (1959).
7. R. PROBER, Transport phenomena in the laminar boundary-layer flow of a multicomponent fluid, Ph.D. Thesis in Chemical Engineering, University of Wisconsin (1961).
8. R. B. BIRD, W. E. STEWART and E. N. LIGHTFOOT, *Transport Phenomena*. Wiley, New York (1960).
9. D. B. SPALDING, A standard formulation of the steady convective mass transfer problem, *Int. J. Heat Mass Transfer* **1**, 192 (1960).
10. H. SCHLICHTING, *Boundary Layer Theory*, 4th Ed. McGraw-Hill, New York (1960).

Résumé—On a utilisé une méthode de perturbation pour obtenir les solutions de couche limite dans le cas d'écoulements sur des dièdres avec faible transport de masse. On arrive à des relations explicites simples entre quantité de mouvement, transport de chaleur et de masse et les conditions à la paroi et dans l'écoulement libre. Les résultats sont donnés pour des nombres de Prandtl et de Schmidt allant de zéro à l'infini et des dièdres d'angles $\beta = 1{,}0$ à $\beta = -0{,}163$.

Zusammenfassung—Lösungen der Grenzschichtgleichung für Keilströmung mit geringem Stoffübergang können nach einer Störmethode erhalten werden. Einfache, explizite Beziehungen ergeben sich zwischen Impuls-, Wärme- und Stoffübergangsanteilen und den Wand- und Freistrombedingungen. Die Ergebnisse sind wiedergegeben für Prandtl- und Schmidtzahlen von Null bis Unendlich und Keilgeometrien von $\beta = 1{,}0$ bis $\beta = -0{,}163$.

Аннотация—В статье используется метод возмущений для получения решений пограничного слоя при обтекании клина в случае малых скоростей переноса массы.

Получены простые точные соотношения между скоростями переноса количества движения, тепла и массы и условиями на границе раздела фаз и свободного потока. Приводятся результаты для чисел Прандтля и Шмидта от нуля до бесконечности и для форм клина при $\beta = 1{\cdot}0$ до $\beta = -0{\cdot}163$.